Extending Firing Rate Models to Include Ionic Effects

by

Tianke Li

University of Pittsburgh, 2019

Submitted to the Graduate Faculty of

the Department of Mathematics in partial fulfillment

of the requirements for the degree of

Bachelor's of Philosophy

University of Pittsburgh

2019

UNIVERSITY OF PITTSBURGH

DEPARTMENT OF MATHEMATICS

This thesis was presented

by

Tianke Li

It was defended on

July 25, 2019

and approved by

Bard Ermentrout, Department of Mathematics

Jonathan Rubin, Department of Mathematics

Jeffrey Wheeler, Departmental of Mathematics

Rachael Neilan, Duquesne University

Thesis Advisor: Bard Ermentrout, Department of Mathematics

Extending Firing Rate Models to Include Ionic Effects

Tianke Li, B.Phil

University of Pittsburgh, 2019

Spiking models have been widely used to describe single neuron oscillation behaviors. However, these models can be quite complex so that in order to incorporate them in networks, one approach is to use so-called firing rate models where the dynamics of the neuron are reduced to the rate at which it fires when presented with a constant stimulus. In pathological conditions such as epilepsy or when the neurons are driven too strongly, they can stop firing due to a phenomenon known as depolarization block, which can come about due to the accumulation of potassium ions in the intracellular space. In the project, we used a well-known Wang-Buzsaki (WB) spiking model but also included an additional equation considering extracellular potassium effects. Given that the extracellular potassium effects is slow and synapses can be reasonably assumed as slow, we applied a slow-fast technique on the WB model and derived a firing rate model describing the synapse-potassium system qualitatively. The bifurcation of the reduced model suggests that the depolarization block threshold can be viewed as the homoclinic bifurcation in the synapse-potassium system, which would be depended upon the potassium sensitivity and the drift rate. In addition, we implement our firing rate model into a two-nearest neighbor spatial model. The spatial-temporal plots suggest our model behavior is consistent with experimental results. The synaptic connectivity has positive effects on seizure propagation and somewhat negative effects on synchronization. On the other hand, the potassium diffusion has a positive influence on synchronization. However, the influence of potassium sensitivity might be more complex. While the neurons under normal physiological conditions can be driven into the seizure-like oscillations in the network, the neurons under depolarization block seem to be a little bit more complicated and require further explanation.

Table of Contents

List of Figures

1.0 Introduction

Neural oscillation is the fundamental mechanism of brain activity, which is driven by either single neuron activities or interactions between neurons. The excitatory and inhibitory neurons interact through neuron currents and extracellular micro-environments, resulting in repetitive patterns of neuron activities ([21]).

An epileptic seizure is defined as a neurological disorder typically caused by neurons that are fired in an abnormal, excessive and synchronized manner, that arise from the decreased inhibition with excessive excitation ([24]). Experimental results suggest that subsequent depolarization block in active fast-spiking neurons provoked large seizure amplitude and propagation of epileptic seizures ([1]). Recent studies have shown that the inhibitory neurons enter depolarization block and stop firing before or during seizure-like activities, which can be a potential motif for the creation of the seizure-like behavior ([31]; [6]). It has been well-known that a large increase in the extracellular potassium is highly associated with the electrographic seizures ([27]; [4]), and the extracellular potassium accumulation may play a casual role in the seizure creation and propagation ([11]). However, the mechanism of how extracellular potassium accumulation may cause neurons to be susceptible to depolarization block is still under examination ([20]; [17]).

Spiking models have been widely used to describe neuron oscillation behaviors. The most famous of these is the Hodgkin-Huxley (HH) model. Hodgkin and Huxley ([14]) created a conductance-based model in order to describe how action potentials are generated and propagated in the squid giant axon. In their model, each neuron is modeled as a circuit diagram, the semipermeable membrane is regarded as a capacitor separating the intracellular environment from the extracellular micro environment, whose capacitance is defined as a constant relating to the property of lipid bilayer. The leak and voltage-gated channels (potassium channel and sodium channel, for example) are modeled as batteries, with such battery resistance referring to the conductance of each channel respectively. The electric potential of the batteries are both dependent on the membrane potential and time, while the conductances are defined as functions of time.

Figure 1: The Circuit diagram of Hodgkin-Huxley Model.

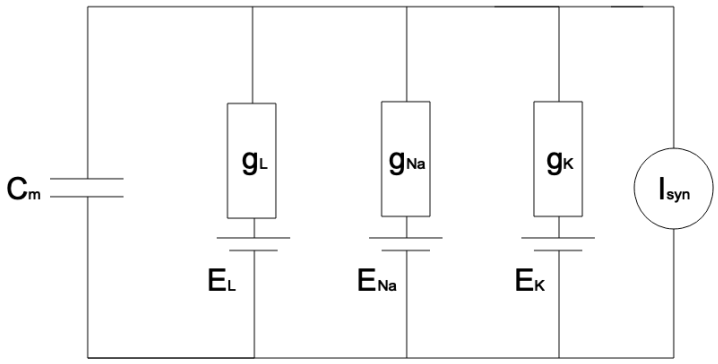

Due to the high complicity of the H-H model, many derivations have been made in order to cooperate with specific conditions. Wang and Buzsaki ([29]) proposed a model taking synaptic inhibition into consideration. Based on the Hodgkin-Huxley model, the researchers structured the synaptic activities by the synaptic current, where the synaptic channels were assumed to be slow comparing to the fast neuronal oscillations. Meanwhile, this model assumed the activation gate of sodium channel to be fast. Consequently, the activation gate was represented by its steady state instead of the kinetic equation.

However, neither of these previous models have taken extracellular microenvironments into consideration. Kim and Nykamp ([17]) investigated the influence of depolarization block on seizure-like activities in the excitatory and inhibitory neuron networks. By creating a Wilson-Cowan ([30]) type model, they applied a bifurcation analysis. Consequently, they found there was a bistability between seizure state and the normal physiological state, which was created by the depolarization block. In addition, they also showed that the extracellular potassium concentration would affect the threshold of depolarization block and would consequently enable the neural network to generate tonic and clonic seizures.

In this study, we investigate the extracellular potassium effects at both the neuron and network level. First, we create a Wang-Buzsaki (WB) type model while taking extracellular potassium effect into consideration to analyze the behavior of single, self-coupled neurons. Next, we derive our reduced firing rate model using slow-fast analysis technique. Afterwards, we put our reduced model into a network and analyze the behavior of the network. Subsequently, the rest of the paper is organized as follows: Chapter 2 explains the way we create

our models, Chapter 3 describes the model results and analysis, and Chapter 4 presents our discussions and conclusions.

2.0 Methods

2.1 Full Model

To started with, we construct a self-coupled single neuron spiking model using a simplified version of the WB model ([29]) while taking extracellular potassium effects into consideration. The model obeys the current balance equation ([14]; [29]; [10]):

$$C_m \frac{dV}{dt} = -I_L - I_{Na} - I_K + I_{syn} + I_0. \tag{2.1}$$

The variables and parameters in the full model are shown in Table 1.

Under the conductance based mechanism ([14]; [29]), the currents can be calculated as :

$$\begin{aligned} I_L &= g_L(V - E_L) \\ I_{Na} &= g_{Na} m^3 h(V - E_{Na}) \\ I_K &= g_K n^4 (V - E_K) \\ I_{syn} &= g_{syn} s V_{drive}. \end{aligned} \tag{2.2}$$

Adopting the Wang-Buzsaki ([29]) mechanism, we assume the activation process of sodium channel was fast and substitute the activation variable m by its steady state, m_∞. The inactivation variable of sodium channel h and the activation variable of potassium n obey the first-order kinetics as following:

$$\begin{aligned} \tau_h \frac{dh}{dt} &= \phi(h_\infty - h) \\ \tau_n \frac{dn}{dt} &= \phi(n_\infty - n) \end{aligned} \tag{2.3}$$

where h_∞ and n_∞ are the steady states of h and n respectively, and τ_h and τ_n are time constants following: $\tau_h = 1.0/(\alpha_h + \beta_h)$ and $\tau_n = 1.0/(\alpha_n + \beta_n)$.

The steady states of the ionic gating variables follow $x_\infty = \frac{\alpha_x}{\alpha_x+\beta_x}$ for any $x \in \{m, n, h\}$ ([14]; [10]). Additionally, the α_x and β_x are defined as:

$$\begin{cases} \alpha_m(V) = \frac{0.1(V+35.0)}{1.0-\exp(-\frac{(V+35.0}{10.0})} \\ \beta_m(V) = 4.0\exp(-\frac{(V+60.0)}{18.0}) \end{cases}$$
$$\begin{cases} \alpha_h(V) = 0.07\exp(-\frac{(V+58.0)}{20.0}) \\ \beta_h(V) = \frac{1.0}{1.0+\exp(-\frac{(V+28.0)}{10.0})} \end{cases} \tag{2.4}$$
$$\begin{cases} \alpha_n(V) = \frac{0.01(V+34.0)}{1.0-\exp(-\frac{(V+34.0)}{10.00})} \\ \beta_n(V) = 0.125\exp(-\frac{(V+44.0)}{80.0}) \end{cases}$$

where V is the membrane potential ([14]; [29]).

Next, we represent the synapses' behavior by the synaptic currents. In addition to the maximal conductance g_{syn} and driving voltage V_{drive}, the synaptic current is also depended upon its gating variable s, which represents the openness of synaptic ion channels. For the computational convenience, we simplify the first order kinetics of the gating variable s as ([29]):

$$\tau_s \frac{ds}{dt} = (a_i(V) - s) \tag{2.5}$$

where the firing function $a_i(V) = \frac{a_i 0}{(1+\exp(-\frac{V-V_{st}}{V_{ss}}))}$.

While the WB model treats the extracellular microenvironment as external and constant, it fails to explain some phenomena such as epilepsy or depolarization block, which might come through the accumulation of extracellular potassium. Taking such effects into consideration, we treat the potassium effects as internal and assumed:

$$\begin{aligned} E_K &= 26.73\log(K/140) \\ \tau_K \frac{dK}{dt} &= (-(K - K_{min}) + \mu_k I_K) \end{aligned} \tag{2.6}$$

2.2 Reduced Model

To develop a firing rate model that includes the effects of potassium accumulation, we take the slow-fast approach in which we assume that the synapse and potassium dynamics are slow compared to the spiking behavior of the neuron. While the latter assumption is reasonable, the assumption of slow synapses is probably not biologically realistic. However, slow synapses are just one way to reduce spiking models to firing rate models ([10]) so one could also adapt a more heuristic approach ([17]). We will stick with the slow-fast approach for simplicity. Let ϵ be small, and the self-coupled WB system can be written as:

$$\begin{aligned} X' &= F(X, s, K) && (2.7)\\ s' &= \epsilon[a_i(V) - s]/\tau_s && (2.8)\\ K' &= \epsilon[\lambda(K_{min} - K) + \mu_K I_K] && (2.9) \end{aligned}$$

where X represents the fast variables, (V, n, h). We first note that since we are using a current-based synapse, we can replace s in the fast equation by, $I = I_0 + g_{syn}V_{drive}s$. where I_0 is applied current. For each pair (I, K) we study the dynamics of the fast system. There are two cases, either there is an equilibrium point, $\bar{X}(I, K)$, or a limit cycle, $\bar{X}(t, I, K)$ with a period, $T(I, K)$. In the former case, we just substitute the equilibrium into the slow dynamics while in the latter case, we do the same but average over the period. Thus we obtain:

$$\begin{aligned} \frac{ds}{dt} &= \epsilon[\bar{a}_i(I, K) - s]/\tau_s && (2.10)\\ \frac{dK}{dt} &= \epsilon[\lambda(K_{min} - K) + \mu_K \bar{I}_K(I, K)]. && (2.11) \end{aligned}$$

Let $\tau = \epsilon t$, then we have $\frac{d}{d\tau} = \epsilon\frac{d}{dt}$. Hence we can simply the equations as:

$$\begin{aligned} \frac{ds}{d\tau} &= [\bar{a}_i(I, K) - s]/\tau_s && (2.12)\\ \frac{dK}{d\tau} &= [\lambda(K_{min} - K) + \mu_K \bar{I}_K(I, K)]. && (2.13) \end{aligned}$$

Our strategy is to numerically compute the averages, $\bar{a_i}$ amd $\bar{I_K}$ over a range of values of I, K and then try to come up with an approximate functional form for the two quantities that will be used to analyze the reduced firing rate/potassium system. The value of parameters are listed in Table 2.

Fixing K at a variety of values between 5 and 15, we increase I and use AUTO in the XPP software to compute the averages. We generally find that for a fixed K, as I increases, the fast system undergoes a saddle-node infinite cycle (SNIC) bifurcation and so the firing rate and other quantities will have a roughly square-root dependence on the applied current ([23]; [10]). For larger K, the magnitude is amplified but, at higher currents, the limit cycle disappears at a Hopf bifurcation and the firing rate goes to zero (as does $\bar{a_i}$). We plot some of these curves in the subsequent chapters.

2.3 Network

Next, we implement our reduced model to further analyze the ionic effect in a network. For simplicity, we create a chain of neurons contains 50 neuron cells, where each neuron cell is coupled with the two other most adjacent neurons ([5]; [10]). Consequently, the synaptic currents and chemical transmitters fired by adjacent cells would also have effects on the neuron, which can be represented as:

$$I_i = i_0 + gV_{drive}((1-2p)s_i + p(s_{i-1} + s_{i+1})) \tag{2.14}$$

where p represents the synaptic connectivity. Due to the complex dynamics of extracellular microenvironment, the synaptic connectivity would not always remain at the highest strength, and is often dependent upon the structure of neuron connection and subjected to synaptic growth ([2]; [19]).

In addition to the synaptic currents, the diffusion effect of extracellular potassium, which is dependent upon its location in the brain and affected by glial cells, also plays an important role in seizure synchronization, as it might be able to redistribute the concentration of

extracellular potassium over the network ([25];[13]). In our model setting, we assume the extracellular potassium could diffuse into the two adjacent cells:

$$K_i' = \lambda(K_{min} - k_i) + \mu_K I_K(I_i, K_i) + q(K_{i+1} + K_{i-1} - 2K_i) \tag{2.15}$$

where q represents the potassium diffusibility.

Lastly, we have the synaptic function derived in our reduced model:

$$\tau s_i' = -s_i + f(I_i, K_i) \tag{2.16}$$

for any $i \in \{1, 2, \cdots, 50\}$ with $s_0 = s_1, s_{51} = s_{50}, K_0 = K_1, K_{51} = K_{50}$. Consequently, we construct our network model, and will try to analyze the influence of synaptic connectivity p, potassium diffusibility q, and the potassium sensitivity μ_k in the network.

Table 1: Variables and parameters in the full model

Variable	Unit	Description
V	mV	Membrane Potential
I_L	μA/cm^2	Leakage current
I_{Na}	μA/cm^2	Sodium current
I_K	μA/cm^2	Potassium current
I_{syn}	μA/cm^2	Synaptic current
E_K	mV	Reversal potential of potassium current
K	mM	The extracellular Potassium Concentration
m		Activating sodium gate
h		Inactivating sodium gate
n		Activating potassium gate
s		Synaptic gate

Parameter	Value	Description
I_0	1 μA/cm^2	Applied current
K_{min}	5 mM	The minimum threshold needed for hyperkalaemia
ϕ	5 s^{-1}	Time constant of gating variables
g_L	0.1 mS	Conductance of leak current
g_{Na}	35 mS	Conductance of sodium current
g_K	9 mS	Conductance of potassium current
g_{syn}	0.2mS	Conductance of synaptic current
E_L	-65mV	Reversal potential of leak current
E_{Na}	35mV	Reversal potential of sodium current
V_{drive}	60mV	Driving voltage of synaptic current
V_{st}	-15mV	Synaptic threshold
V_{ss}	1mV	
a_i0	1	
μ_k	0.3	Potassium sensitivity
τ_s	1000ms	Time constant of synapse
τ_k	1000ms	Time constant of extracellular potassium

Table 2: parameters in the reduced model and network

Parameter	Value	Description
I_0	0 μA	Applied current
K_{min}	5 mV	The threshold of hyperkalaemia
g_{syn}	0.2mS	Conductance of synaptic current
μ_k	0.2	Potassium sensitivity
τ_s	1	Time constant of synapse
λ	1	Drift rate

3.0 Results

3.1 Full Model

We simulate the WB spiking model in order to analyze the extracellular potassium effect on the depolarization block of self-excitatory neurons.

To start with, we investigate the voltage changes of self-excitatory neurons over time under different potassium sensitivities μ_k. Figure 2a and 2b show that under normal conditions, an increase in the potassium build up ability would reduce the amplitude of neuron oscillation. As the potassium build up increases, Figure 2c suggests the condition that generates seizure-like oscillations. With continuing increase in the potassium build up, the period of seizure-like oscillation increases until it reaches a full depolarization block as Figure 2d suggested.

Figure 2: Voltage behavior over time.

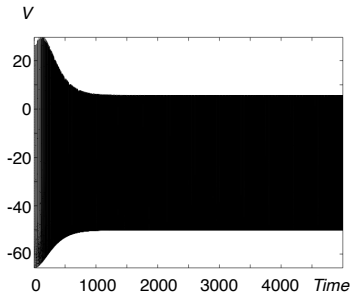

a: $\mu_K = 0.1$, the normal physiological condition

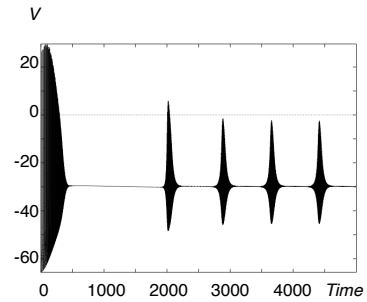

c: $\mu_K = 0.3$, seizure-like bursting have been generated

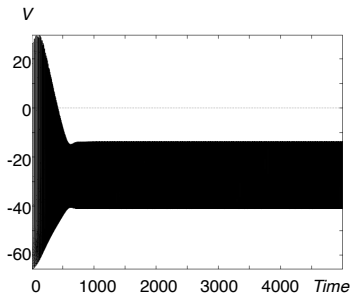

b: $\mu_K = 0.2$, normal physiological condition, with lower amplitude

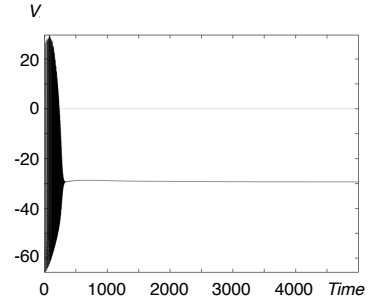

d: $\mu_K = 0.4$, the pathological condition, depolarization block generated

Next, we analyze the behavior of extracellular potassium and synapse over time. The results are shown in Figure 3, where Figure 3a illustrates the behavior happens in the extracellular potassium while Figure 3b illustrates the behavior happen in synapses firing level. The red, green, blue and purple lines are representing the cases of $\mu_K = 0.1, 0.2, 0.3, 0.4$ respectively. The initial condition has been set at the normal condition which keeps the potassium at 5mM and the synapse also fires at the normal level. As we can see from the Figure 3a, with the increase in the sensitivity, the reverse potential of extracellular potassium has reached to higher levels. In particular, under the seizure-like bursting conditions (as the blue curve suggested, when $\mu_k = 0.3$), we can observe a slow oscillation in the reverse potential of the potassium. When the depolarization happens (as the purple curve suggested,when $\mu_K = 0.4$), the reverse potential of potassium gradually goes down to a fixed level and remains there.

On the other hand, the synaptic firing level keeps dropping as the sensitivity increases. Similar to the potassium, under the seizure-like conditions (the blue curve), we can also observe a slow oscillation in the firing level of synapses. Additionally, we find that under the depolarization block conditions, the synapses stop firing (the purple curve).

Figure 3: Potassium and synapses behavior over time under different conditions.

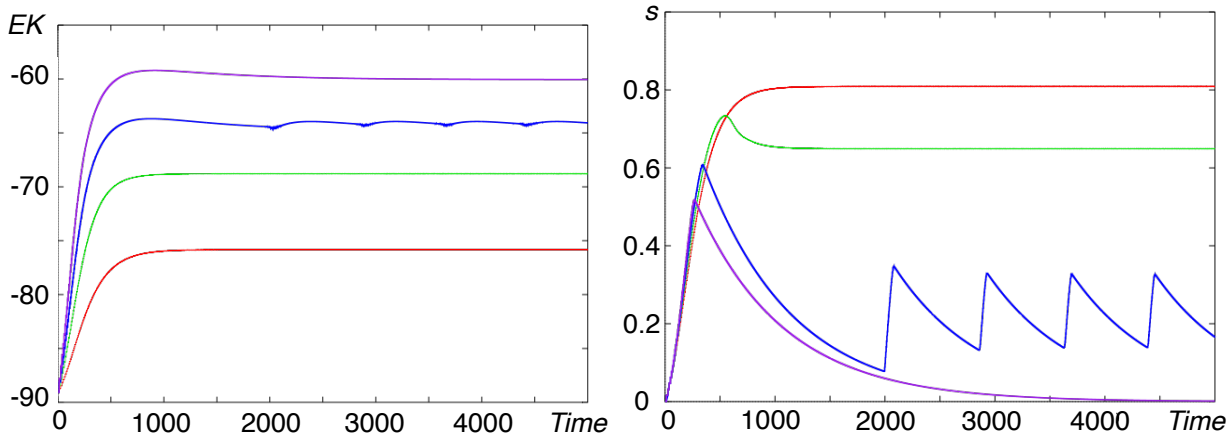

a: Extracellular potassium over time

b: Synapse activation over time

3.2 Reduced Model

As we have discussed in the previous chapter, by applying fast slow analysis, we can treat these slow factor as parameters in our full model. In addition, since we are using the current-based model, we have our input current of firing rate as $I = I_0 + g_{syn}V_{drive}s$. Consequently, it is sufficient for us to just look at the variables I and K.

As mentioned in Chapter 2.2 , we approximate the average function of potassium current and the synaptic firing rate. Thus, treating the input current I and potassium concentration K as parameters, we are able to compute the functions of $\bar{I_K}$ and $\bar{a_i}$. Using bifurcation analysis, we calculated the average of I_K and a_i functions over I under different K conditions, and then we fitted this functions by hand. Some fitting results are shown below:

Figure 4: Some Fitting Results

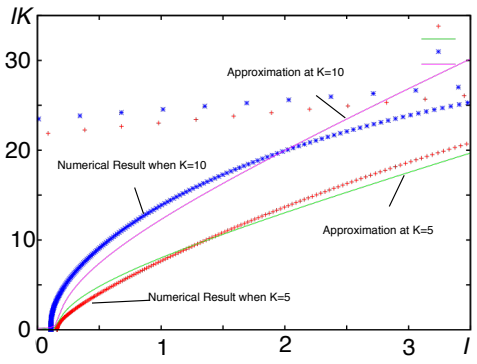

a: Fitting results of $\bar{I_K}$

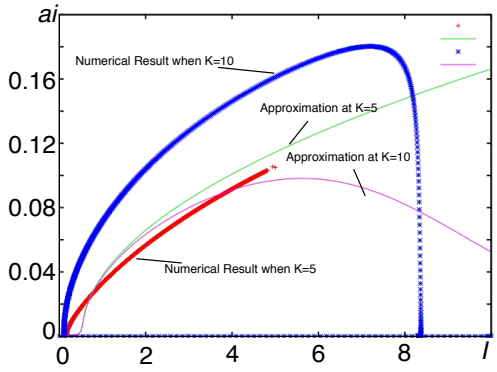

b: Fitting results of $\bar{a_i}$

We firstly fix $K = 5$mM and create the bifurcation of $\bar{I_K}$ over I. We fit the equation with the function:

$$g_5(I) = 7.95\sqrt{smax(I - 0.16) + 0.25smax(I - 0.16)^2} \tag{3.1}$$

where $smax$ is a smoothed positive part function.

In addition, we find that the potassium has a modulation effect on the amplitude which is depends on the potassium concentration level. Therefore, we fix $I = 1\mu$A and come up

with the function of $\bar{I_K}$ dependence on K to be:

$$amp_0(K) = 6.8 + \frac{28}{1 + \exp(-0.6(K - 13))}. \tag{3.2}$$

By scaling the potassium influence on the amplitude $amp(K) = amp_0 K / amp_0(5)$, we came up with our approximation function of $g_k(I, K)$ of $\bar{I_K}$:

$$g_k(I, K) = g_5(I) amp(K) \tag{3.3}$$

Figure 4a provides some the fitting results when $K = 5$ and $K = 10$. The numerical computation results are listed in dotted lines while our approximation are represented by solid lines. As we can see from the figure, both the approximation at $K = 5$mM (the green curve) and at $K = 10$mM (the purple curve) are fairly close to the numerical results.

On the other hand, our approximation of a_i in Figure 4b might not be viewed as a good fitting at the first glance, but it does reflect the synaptic firing rate qualitatively. As we discussed in the previous chapter 2.2, the cut-off threshold for the fast system at the Hopf bifurcation over K is fairly accurately modeled with the function:

$$\hat{I}(K) = -\log(K/14.5)/0.44. \tag{3.4}$$

As we can see from Figure 5, our approximation (the red curve) fits almost perfectly with the numerical simulation results (the blue dotted curve), which separates the firing cases from the cases of depolarization block. In addition, as we mentioned in the previous Chapter 2.2, the synaptic firing rate has an approximately square-root dependence on the input current I. Therefore, we constructed our approximation function $f(I, K)$ of $\bar{a_i}$ as:

$$f(I, K) = \frac{0.054\sqrt{smax(I - 0.51)}}{(1 + \exp(0.5(I - \hat{I}(K))))} \tag{3.5}$$

Figure 5: The approximation of the fast-system Hopf bifurcation threshold.

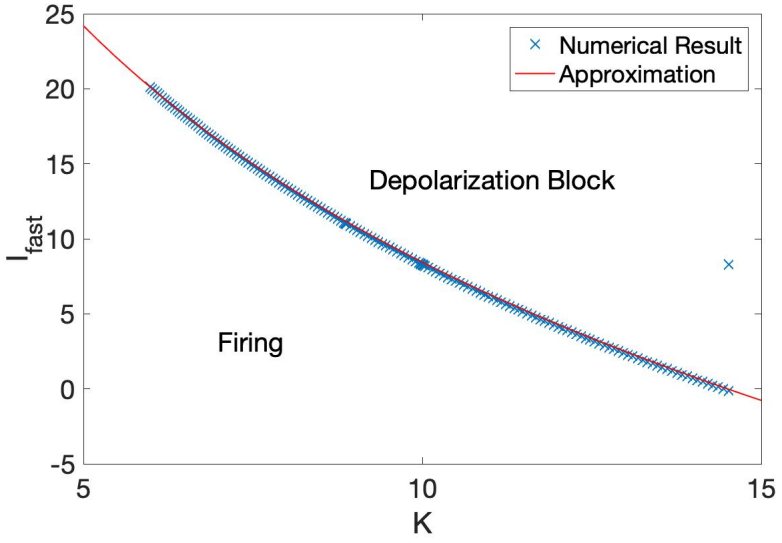

Next, with the approximation functions in hand, we look at the s-K system. The first step is to analyze the system behavior through phase plane. We start with the normal physiological condition (Figure 6a), where the extracellular potassium and synapses firing rate are maintained at a stable rate (at stable equilibrium). With the increase in the potassium sensitivity μ_K, the fixed point moves towards a higher potassium concentration K and lower firing rate s, which reveals the findings we have found in the full model (not shown in the figure). When the μ_K passes some threshold, a stable limit cycle gradually emerged (Figure 6b), suggesting there might exist a supercritical Hopf bifurcation in the system. Progressively, such limit cycle enlarges with the increase in the in potassium sensitivity, and unstable limit cycle can be observed. Figure 6c is an example under such conditions, where inner red curve is the stable limit cycle, and the outer blue curve is the unstable limit cycle. The points start inside the unstable cycle all converges towards the stable limit cycle, while the ones outside the unstable limit cycle directly goes towards the other fixed point which demonstrates the depolarization block condition. In addition, with the increase in the μ_k, the stable and unstable limit cycles get together. However, when the μ_k passed through some other threshold, both limit cycles disappear and all the points converge to a fixed point

(Figure 6d), which might be caused by a homoclinic bifurcation.

Figure 6: Phase planes of the s-K system

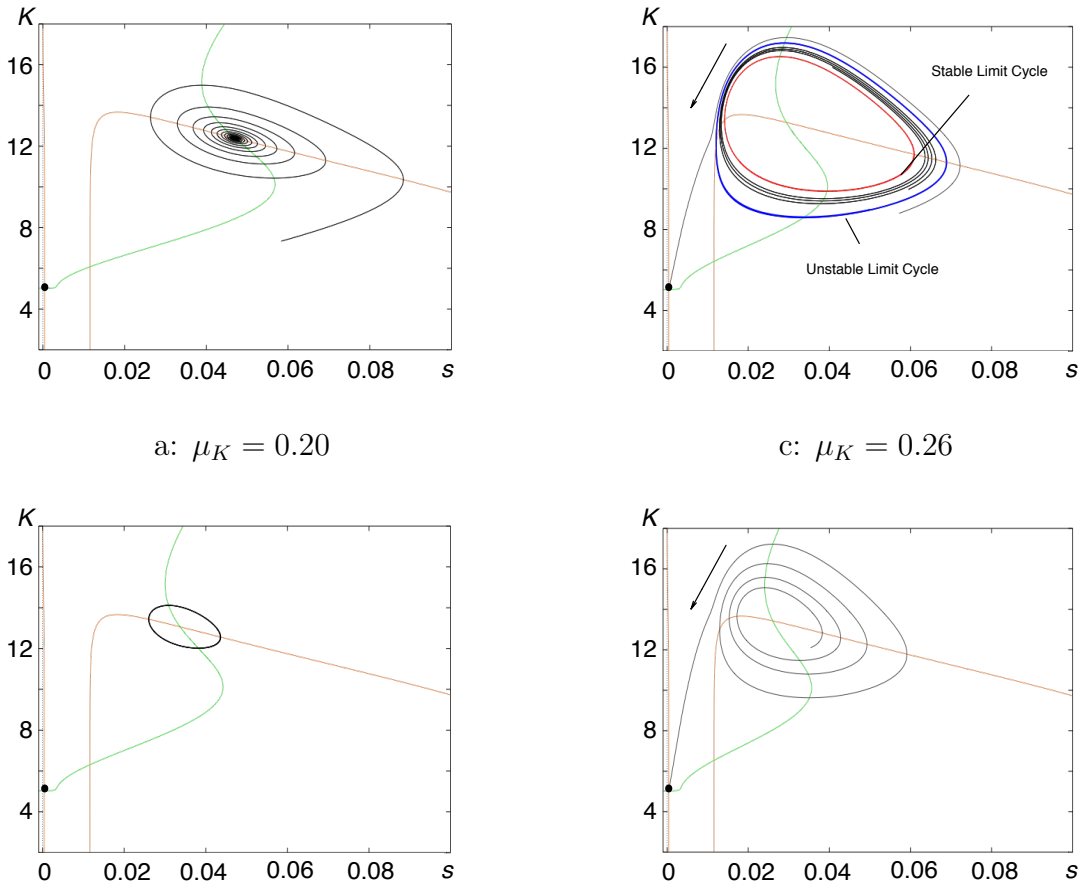

a: $\mu_K = 0.20$

c: $\mu_K = 0.26$

b: $\mu_K = 0.24$

d: $\mu_K = 0.28$

The bifurcation diagram over μ_k provides support to such hypothesis, as we can see in Figure 7. In the figure, the red curve represents the stable branch, the black curves represent the unstable branch, the green dotted curves represent the stable limit cycle, and the blue curves represent the unstable limit cycle. A supercritcal Hopf bifurcation (the upper curve) intersects with the saddle-node bifurcation (the lower curve). Consequently, we can see that when μ_k initially increases from the physiological phase (the red curve), the synaptic firing rate goes down along the red curve. When it passes some threshold, a supercritical Hopf bifurcation happens and creates the stable and unstable limit cycles. But when the unstable

limit cycle reaches the homoclinic bifurcation, the limit cycles disappear and jumps to the fixed point of depolarization block.

Figure 7: The bifurcation diagram over μ_k.

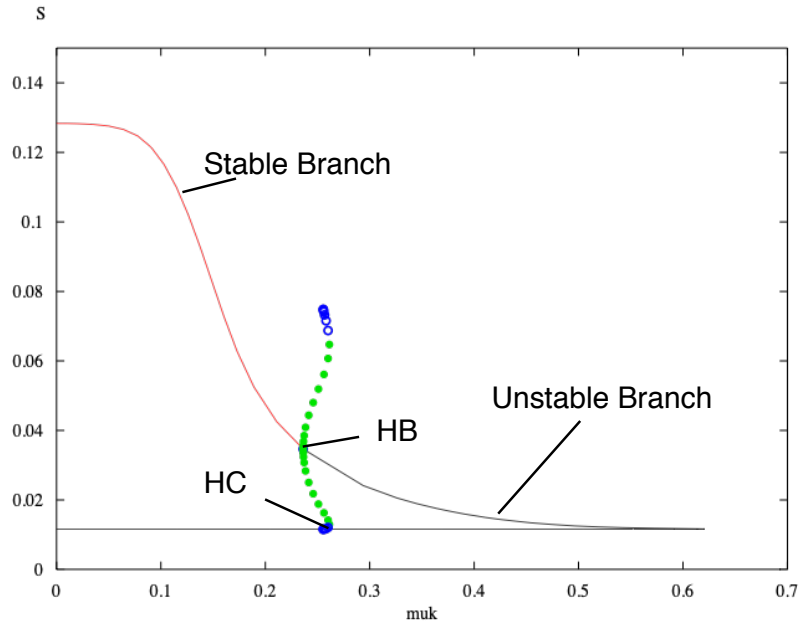

Besides μ_k, the drift rate λ also has strong impacts on the concentration of extracellular potassium, and shapes the s-K system accordingly. While all of our previous works assume that $\lambda = 1$, we conduct the bifurcation diagram of λ over μ_k (Figure 8a) to try to analyze such effects. While the blue curve represents the Hopf bifurcation, the black line is when the Hopf bifurcation joining stable and unstable limit cycles (the SNIC bifurcation). Therefore, the region between these two curves should contain some bistability. For illustration purposes, we create three phase planes, representing the Region 1 (Figure 8b), Region 2 (Figure 8c) and Region 3 (Figure8d) of the bifurcation diagram (Figure 8a) respectively. As we can see from these figures below, in the Region 1 above the blue curve (Figure 8b), the equilibrium is at a fixed point which behaves similar to the physiological condition. On the other hand, the Region 3 below the black curve (Figure 8d) has an equilibrium at a fixed point that synapses stop firing, which behaves similar to the depolarization block. Meanwhile, the Region 2 in the middle generates stable limit cycles, as our Figure 8c suggested.

Figure 8: The effects of λ

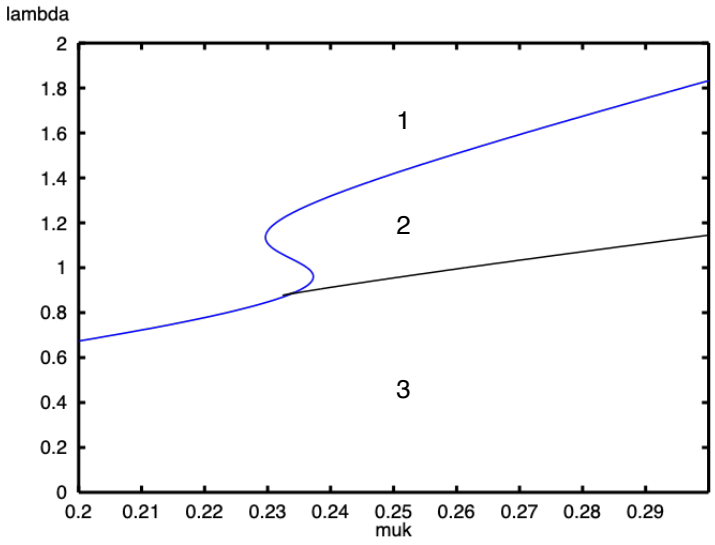

a: bifurcation diagram of λ over μ_k

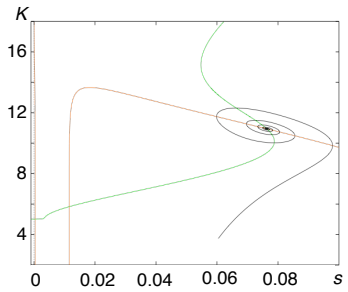

b: $\mu_k = 0.25$, $\lambda = 1.6$

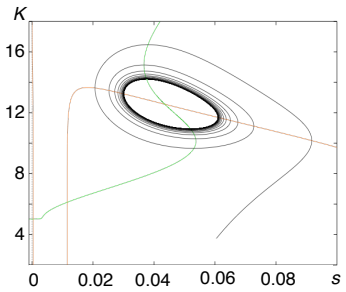

c: $\mu_k = 0.25$, $\lambda = 1.2$

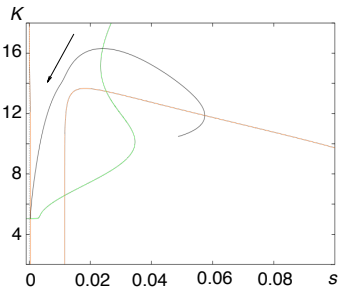

d: $\mu_k = 0.25$, $\lambda = 0.7$

3.3 Network

The next step is to analyze the potassium effect in a neural network. For simplicity, we create a neural network that only considers their closest neighbors effect. By manipulating the parameters considering potassium diffusion, synaptic connectivity and potassium sensitivities, we analyze their effects in the 2-nearest neighbor spatial model. The results are

shown as the spatial-temporal plots in Figure 9, 10 and 11, where the horizontal axis is space illustrating the seizure propagation and the vertical axis is time illustrating the changes in the seizure behavior. The colors at each point represent the average firing level of the neuron (between 1 and 0.1) at the specific time point and are explained using the color map, where the dark blue represents the cases when neurons stop firing.

3.3.1 Synaptic Connectivity

Figure 9a and Figure 9b illustrates the effect of synaptic connectivity given the other variables fixed. As we can see from these two plots, the synaptic connectivity both affects the speed of seizure spread and synchronization. In particular, a higher synaptic connectivity may results in a faster speed of spread and a weaker synchronization. For instance, if we fix the potassium diffusion at $q = 0.01$, comparing the synaptic connectivity $p = 0.12$ (Figure 9a) with $p = 0.15$ (Figure 9b), one can clearly see a less steep slope for Figure 9b, suggesting it takes less time to propagate the oscillation to the next cell. Meanwhile, a less clear horizontal line suggests it mediates the synchronization effect. Moreover, as we can see in the Figure 9b, when the synaptic mediation effect is relatively significant, the cells in the middle part has much less synchronization comparing to the ones on the edges, but such effects also gradually depletes over time.

Figure 9: Spatial-temporal plots under different synaptic connectivity

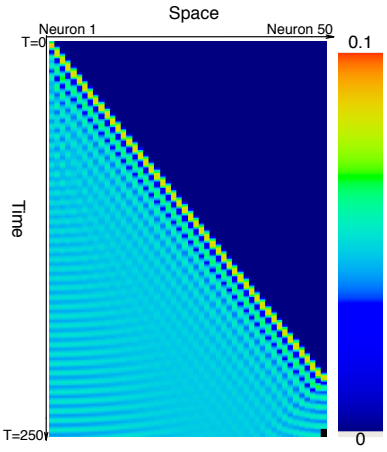

a: $p = 0.12, q = 0.01, \mu_K = 0.2$

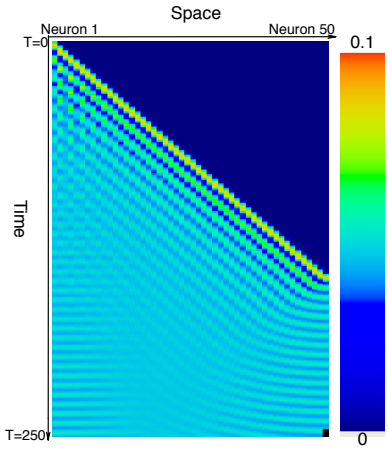

b: $p = 0.15, q = 0.01, \mu_K = 0.2$

3.3.2 Potassium Diffusion

On the other hand, the potassium diffusion plays a relatively minor role comparing to synaptic connectivity. As Figure 10a and Figure 10b suggested, a higher potassium diffusion results in a faster speed of synchronization, given the synaptic connectivity is fixed. To be more specific, Figure 10 fixes the synaptic connectivity at $p = 0.2$ and compares the potassium diffusion of $q = 0.08$ (Figure 10a) and $q = 0.2$ (Figure 10b). As we can see clearly, when the potassium diffusion is low (Figure 10a), there will be little interactions between cells except through synaptic firing, and each neuron are firing individually without clear horizontal synchronization lines. Therefore, the cells are not very likely to synchronize. However, when the potassium diffusion is high (Figure 10b), the cells will be able to communicate with their neighbors quickly and hence the synchronization will be enhanced, as the clear horizontal synchronization line suggested. When the potassium diffusion is strong, the neurons in the middle of the chain would more likely to have a period of continuous spiking (constant firing rate over time), but such behavior would gradually replaced by the synchronized oscillations, which has been shown in our Figure 10b.

Figure 10: Spatial-temporal plots under different potassium diffusibility

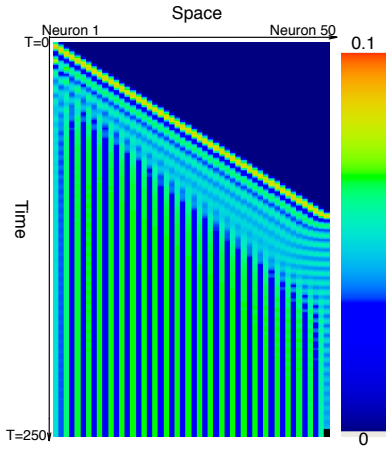

a: $p = 0.2, q = 0.08, \mu_K = 0.2$

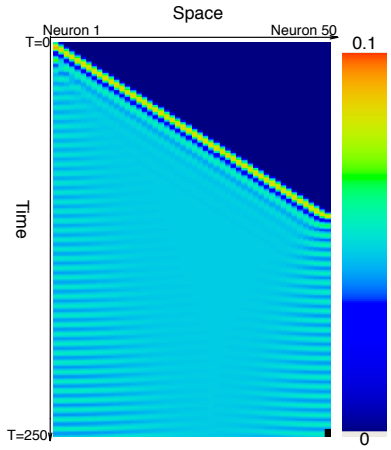

b: $p = 0.2, q = 0.2, \mu_K = 0.2$

3.3.3 Potassium Sensitivity

The dynamics of potassium sensitivity seem to be a little more complex than the other two. While the initial neurons in previous sections are assumed to undergo seizure-like activities, we are trying to address the potassium sensitivity effect and analyze the networks given the different phases that the neurons might be in. We listed two representative patterns we have found in the Figure 11. Figure 11a shows the network pattern for neurons under normal physiological conditions. Given a strong potassium diffusion effect, some neurons may also undergo a seizure-like oscillation. However, possibly with dominant synaptic connectivity effect, the seizure synchronization effect is fairly weak. On the other hand, pathological neurons may result prior neuron cells into infrequent oscillation through backward propagation and create chaotic patterns, as Figure 11b suggested. Such effect might result from that the potassium diffusion reduces local potassium concentration. However, it is also possible to be resulted from the discrepancy in our model that the concentration of extracellular potassium is lower than expected under depolarization block conditions, since our reduced model only able to capture the lower fixed point rather than the bistability of the depolarization block.

Figure 11: Spatial-temporal plots for different potassium sensitivity

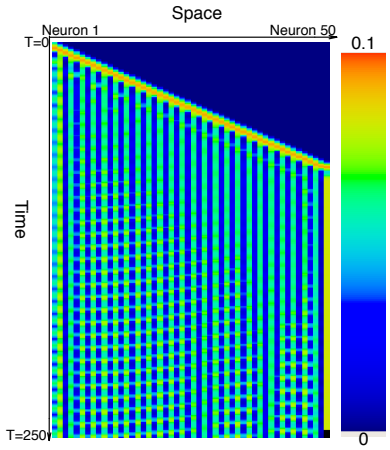

a: $p = 0.3, q = 0.01, \mu_K = 0.18$

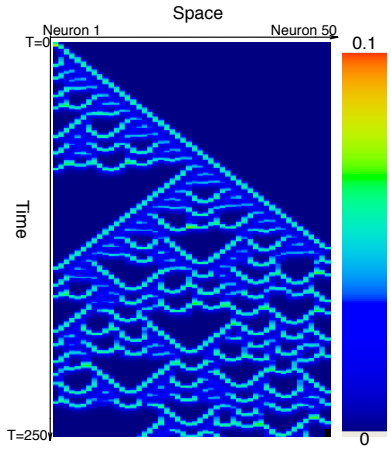

b: $p = 0.2, q = 0.2, \mu_K = 0.3$

4.0 Discussion

4.1 Conclusion

This project has explored the mechanism of the extracellular potassium affecting epilepsy creation at both single cell and neuron network levels. Our WB type model has shown that given all other conditions to be the same, the increase in the sensitivity of the potassium channels may drive normal fast-spiking neuron cells to create slow seizure-like oscillations or depolarization block (Figure 2). In addition, such increase in the potassium sensitivity would depress the synapses firing and result in a rise of extracellular potassium concentration, which consequently affect the threshold of depolarization block (Figure 3). We analyze such phenomena in more detail using our reduced model, which is created through the slow-fast analysis and captures the dynamic system qualitatively. By conducting bifurcation analysis over μ_K, we found there exists a Hopf bifurcation intersects with a saddle-node bifurcation, creating a bistability of the system (Figure 7). To be more specific, given that synapses are firing above the threshold, increasing extracellular potassium sensitivity from physiological conditions initially creates the limit cycles that portrays seizure-like oscillations through a supercritical Hopf bifurcation. Progressively, such limit cycles enlarge along with μ_K until it reaches the homoclinic bifurcation where the limit cycle is destroyed. Consequently, the system rests in a fixed point which represents the depolarization block. Additionally, we looked further into how the relationship between λ and μ_K affect the bistability (Figure 8), which helps to improve the understanding of seizure generation.

Besides, our firing rate model also helps to explain neural behavior in the network. In our 2-nearest neighbor networks, given that the first activated neuron undergo a seizure-like activity, the synaptic connectivity has positive influence on seizure propagation but negative influence on the synchronization (Figure 9). On the other hand, the potassium diffusion only has positive influence on the synchronization (Figure 10). Besides, the potassium diffusion and synaptic connection seem to have backpropagation effect onto the network, but such effect behaves differently depending on the state of the first activated neuron (Figure 11).

If the neuron is in the normal state, the network still is able to be activated and performs somewhat seizure-like. On the other hand, if the neuron is in the depolarization block, the network behaves a little strange, which may also result from the back-propagation effect of synaptic connection and potassium diffusion.

4.2 Comparing to Experimental Results

Many previous *in vitro* studies analyzing extracellular potassium effects on epilepsy started with increasing the extracellular potassium concentration and applying initial current onto the neurons ([25]; [4]; [3]). However, due to the complicated dynamics in neural activities, the effect of extracellular potassium is somewhat controversial. Early researchers concluded that the extracellular potassium have little influence seizure generations ([15]; [12]; [22]). Such conclusions might be true under normal physiological conditions, but when the concentration exceed the threshold, it might affect the membrane depolarization, create alternations in synaptic functions and cause the depolarization block ([25]; [4]) in the seizure-like neurons. However, the depolarization block threshold of the extracellular potassium concentration might be too hard to compute ([25]; [3]; [17]). Such phenomenon is coherent with our bifurcation results, as the threshold is not solely depended upon the concentration but other factors such as potassium sensitivity and the drift rate. In addition, some abnormalities, such as high extracellular potassium concentration in the absence of neuronal firing ([4]) or the elevation of extracellular potassium concentration from bursting to seizure-like ([9]) can also be revealed through our full model. Consequently, our model results provide theoretical evidence to the hypothesis that the extracellular potassium concentration, though highly correlated with epileptic seizures, might not be the only cause of the depolarization block, as the potassium sensitivity plays a key role in the bifurcation structure.

In addition, our model helps to explain some seizure activity in neural network. For instance, the synaptic remodeling and reorganization is widely seen during the epileptogenesis period ([7]; [2]; [19]), which results in an increase in the synaptic connectivity. The seizure spread concurs with our finding that the increase in synaptic connectivity would enhance the

seizure propagation. Besides, our results suggest that the increase in synaptic connectivity in neurons diminishes the seizure synchronization, which coincides with the clinical and experimental results that synaptic remodeling or the GABA release can be used in mediating seizure synchronization in neocortex ([6]; [2]; [19]).

The diffusion effect of extracellular potassium, though its exact role remains unclear, is considered to be related to the seizure synchronization, and such effects may be depended upon the spatial structure ([18]; [26];[13]). Our model results support the conclusion that the potassium diffusion accelerates the seizure synchronization process, while its effects on propagation are not clearly seen in our model. Furthermore, our model helps to explain that the neurons in the network are more susceptible towards seizure-like oscillation and depolarization block. Nonetheless, our model is generally coherent with the experimental findings and contributes to the understanding of epileptogenesis.

4.3 Comparing to Other Computational Models

Since the extracellular microenvironment has complex feedback loops interacting with neurons and might be too hard to be studied experimentally ([13]), many computational models have been constructed to analyze such issues.

Earlier research have shown that the changes of ion concentration would affect the ion currents and membrane potentials, which consequently influence the epileptiform neuronal behavior, though the exact role of extracellular potassium remains controversial ([28]; [16]). The potassium diffusion ability, the strength of sodium-potassium pumps and the glial cells ability of clearing up extracellular potassium in the single neuron model may all create seizure-like slow oscillations and depolarization block when only ion concentration effects are considered in the model ([8]). The model reveals the importance of extracellular potassium clearing up ability, which in our model is represented by the potassium sensitivity μ_k. And our result is consistent with their findings. The higher potassium sensitivity drives normal neurons into the seizure-like phase through a homoclinic bifurcation and gradually results in the depolarization block through a Hopf bifurcation.

However, Cressman's model does not take the chemical communication between neurons into consideration, where synaptic firing plays an important role in seizure propagation and synchronization observed in experimental findings ([13]). Accordingly, Bacak construct a conductance-based model that both the potassium current and the leakage current are dependent on extracellular potassium concentration, and examines the bursting patterns when synaptic interactions are blocked ([3]). It turns out that the endogenous bursting can not be observed under such circumstances. Hence, the effects of extracellular potassium might be plausible under the *in vivo* physiological conditions, and additional conditions such as synaptic excitability should be taken into consideration ([3]). The finding in Bacak's model reveals the importance of synaptic communications. Consequently, we represent the synaptic communication by the synaptic firing rate, generalizing the use of our model to fit for the *in vivo* cases.

Still, the model constructed by Bacak ([3]) does not provide any insightful explanation of extracellular potassium mechanism. Kim and Nykamp ([17]) constructed models describing the bifurcation structure of the seizure-like activities resulting from depolarization block in the neurons. They found that the physiological and seizure-like states can co-exist, where the seizure-state may occur through saddle-node or homoclinic bifurcation. Such feature is also captured in our model. In addition, they proposed that the threshold of depolarization block is affected by the extracellular potassium concentration, which is further explained through our model. Instead of the extracellular potassium concentration, the threshold of depolarization block can be revealed as the homoclinic bifurcation point in the s-K system, hence should be depended up on the potassium sensitivity. In addition, since the region of bistablity is related with the λ, its value should also have impacts on the bifurcation structure and consequently regulates the threshold of depolarization block.

4.4 Limitations and Further Research

Our models provide insights of the mechanism of extracellular potassium and contribute to the understanding of epileptogenesis. Even so, there are a few improvements and further

research can be made based on our work. The first thing is the fitting accuracy. As one may notice, the amplitude of the oscillations might be larger than the reasonable scale under either *in vitro* or *in vivo* conditions. Such discrepancy might result from our hand-fitted current functions, which generally captured the shape of the real data, but the actual fitting might need to be improved. Besides, the neuronal networks in realistic biological settings are weigh more complicated than a chain where only two nearest neighbors can influence a neuron, hence some other models, such as a full connected network or other type networks can also be analyzed using our approaches.

In addition, the concentration of extracellular potassium under depolarization block in our reduced model might be lower than some *in vitro* experiments suggested. Our model is only capable to capture the lower node but not able to reveal the bistability of the depolarization block. Such phenomena result from the complicated influence of the initial applied current I_0, which requires further analysis. Consequently, our analysis of the network under depolarization block conditions might not be exact.

Bibliography

[1] Omar Ahmed, Mark Kramer, Wilson Truccolo, Jason S Naftulin, Nicholas Potter, Emad Eskandar, Garth R Cosgrove, Andrew Blum, Leigh Hochberg, and Sydney S Cash. Inhibitory single neuron control of seizures and epileptic traveling waves in humans. *BMC Neuroscience*, 15:F3, 07 2014.

[2] Klaus Albus, Uwe Heinemann, and Richard Kovács. Network activity in hippocampal slice cultures revealed by long-term in vitro recordings. *Journal of Neuroscience Methods*, 217(1):1 – 8, 2013.

[3] Bartholomew J. Bacak, Joshua Segaran, and Yaroslav I. Molkov. Modeling the effects of extracellular potassium on bursting properties in pre-bötzinger complex neurons. *Journal of Computational Neuroscience*, 40(2):231–245, Apr 2016.

[4] Marom Bikson, Philip J. Hahn, John E. Fox, and John G.R. Jefferys. Depolarization block of neurons during maintenance of electrographic seizures. *Journal of Neurophysiology*, 90(4):2402–2408, 2003. PMID: 12801897.

[5] György Buzsáki. *Rhythms of the brain*. Oxford University Press, 2011.

[6] Mario Cammarota, Gabriele Losi, Angela Chiavegato, Micaela Zonta, and Giorgio Carmignoto. Fast spiking interneuron control of seizure propagation in a cortical slice model of focal epilepsy. *The Journal of Physiology*, 591(4):807–822, 2013.

[7] Yunxiang Chu, Xiaoming Jin, Isabel Parada, Alexei Pesic, Beth Stevens, Ben Barres, and David A. Prince. Enhanced synaptic connectivity and epilepsy in c1q knockout mice. *Proceedings of the National Academy of Sciences*, 107(17):7975–7980, 2010.

[8] John R. Cressman, Ghanim Ullah, Jokubas Ziburkus, Steven J. Schiff, and Ernest Barreto. The influence of sodium and potassium dynamics on excitability, seizures, and the stability of persistent states: I. single neuron dynamics. *Journal of Computational Neuroscience*, 26(2):159–170, Apr 2009.

[9] Christopher A. Del Negro, Sheree M. Johnson, Robert J. Butera, and Jeffrey C. Smith. Models of respiratory rhythm generation in the pre-bötzinger complex. iii.

experimental tests of model predictions. *Journal of Neurophysiology*, 86(1):59–74, 2001. PMID: 11431488.

[10] G. Bard. Ermentrout and David H. Terman. *Mathematical foundations of neuroscience*. Springer Science Business Media, 2010.

[11] Allen P. Fertziger and James B. Ranck. Potassium accumulation in interstitial space during epileptiform seizures. *Experimental Neurology*, 26(3):571 – 585, 1970.

[12] Robert S. Fisher, Timothy A. Pedley, Jr Moody, William J., and David A. Prince. The role of extracellular potassium in hippocampal epilepsy. *JAMA Neurology*, 33(2):76–83, 02 1976.

[13] Flavio Fröhlich, Maxim Bazhenov, Vicente Iragui-Madoz, and Terrence J. Sejnowski. Potassium dynamics in the epileptic cortex: New insights on an old topic. *The Neuroscientist*, 14(5):422–433, 2008. PMID: 18997121.

[14] A. L. Hodgkin and A. F. Huxley. A quantitative description of membrane current and its application to conduction and excitation in nerve. *The Journal of Physiology*, 117(4):500–544, 1952.

[15] J.R. Hotson, G.W. Sypert, and A.A. Jr. Ward. Extracellular potassium concentration changes during propagated seizures in neocortex. *Experimental Neurology*, 38(1):20 – 26, 1973.

[16] H. Kager, W. J. Wadman, and G. G. Somjen. Simulated seizures and spreading depression in a neuron model incorporating interstitial space and ion concentrations. *Journal of Neurophysiology*, 84(1):495–512, 2000. PMID: 10899222.

[17] Christopher M. Kim and Duane Q. Nykamp. The influence of depolarization block on seizure-like activity in networks of excitatory and inhibitory neurons. *Journal of Computational Neuroscience*, 43(1):65–79, Aug 2017.

[18] Jun Lian, Marom Bikson, Jianwei Shuai, and Dominique M. Durand. Propagation of non-synaptic epileptiform activity across a lesion in rat hippocampal slices. *The Journal of Physiology*, 537(1):191–199, 2001.

[19] Kyle P. Lillis, Zemin Wang, Michelle Mail, Grace Q. Zhao, Yevgeny Berdichevsky, Brian Bacskai, and Kevin J. Staley. Evolution of network synchronization during

early epileptogenesis parallels synaptic circuit alterations. *Journal of Neuroscience*, 35(27):9920–9934, 2015.

[20] William J. Moody, Kin J. Futamachi, and David A. Prince. Extracellular potassium activity during epileptogenesis. *Experimental Neurology*, 42(2):248 – 263, 1974.

[21] E. Neustadter, K. Mathiak, and B.I. Turetsky. Chapter 13 - eeg and meg probes of schizophrenia pathophysiology. In Ted Abel and Thomas Nickl-Jockschat, editors, *The Neurobiology of Schizophrenia*, pages 213 – 236. Academic Press, San Diego, 2016.

[22] TA Pedley, RS Fisher, KJ Futamachi, and DA Prince. Regulation of extracellular potassium concentration in epileptogenesis. *Federation proceedings*, 35(6):1254—1259, May 1976.

[23] John Rinzel and G. Bard Ermentrout. Methods in neuronal modeling. chapter Analysis of Neural Excitability and Oscillations, pages 135–169. MIT Press, Cambridge, MA, USA, 1989.

[24] Vikram G. Shakkottai and Catherine Lomen-Hoerth. *Nervous System Disorders*. McGraw-Hill Education, New York, NY, 2019.

[25] G G Somjen. Extracellular potassium in the mammalian central nervous system. *Annual Review of Physiology*, 41(1):159–177, 1979. PMID: 373587.

[26] Mircea Steriade and Igor Timofeev. Neuronal plasticity in thalamocortical networks during sleep and waking oscillations. *Neuron*, 37(4):563–576, Feb 2003.

[27] Eva Syková, Tomáš Mazel, Lýdia Vargová, Iban Voříšek, and Šárka Prokopová-Kubinová. Extracellular space diffusion and pathological states. In *Volume Transmission Revisited*, volume 125 of *Progress in Brain Research*, pages 155 – 178. Elsevier, 2000.

[28] A. van Harreveld. Two mechanisms for spreading depression in the chicken retina. *Journal of Neurobiology*, 9(6):419–431, 1978.

[29] Xiao-Jing Wang and György Buzsáki. Gamma oscillation by synaptic inhibition in a hippocampal interneuronal network model. *Journal of Neuroscience*, 16(20):6402–6413, 1996.

[30] Hugh R. Wilson and Jack D. Cowan. Excitatory and inhibitory interactions in localized populations of model neurons. *Biophysical Journal*, 12(1):1–24, Jan 1972.

[31] Jokubas Ziburkus, John R. Cressman, Ernest Barreto, and Steven J. Schiff. Interneuron and pyramidal cell interplay during in vitro seizure-like events. *Journal of Neurophysiology*, 95(6):3948–3954, 2006. PMID: 16554499.